Distortions from the Tetragonal $HfCuSi_2$-Type Structures to the Orthorhombic $GdCuAs_{1.15}P_{0.85}$-Type Structures in $REMX_2$ (RE = Rare Earth; M = Cu, Ag; X = P, As, Sb): Mismatch between the Sizes of the M and X Atoms

Yurij Mozharivskyj and Hugo F. Franzen*

Department of Chemistry and Ames Laboratory of US DOE, Spedding Hall, Iowa State University, Ames, Iowa 50011

Received: March 1, 2002

The $RECuAs_{2-x}P_x$ phases undergo symmetry-breaking transitions from tetragonal $HfCuSi_2$-type structures ($P4/nmm$ space group) to orthorhombic $GdCuAs_{1.15}P_{0.85}$-type structures ($Pmmn$ space group) upon substitution of arsenic by phosphorus. According to Landau theory, the distortions correspond to the B_{1g} irreducible representation and can be continuous. The $P4/nmm \rightarrow Pmmn$ transitions are not caused by a Peierls-like instability of the square As/P nets but result from a structural adaptation for the smaller P atoms. The stability of the tetragonal $RECuAs_{2-x}P_x$ and other $REMX_2$ structures with respect to the orthorhombic distortion can be characterized by a relative interatomic distance in the As/P or X layer. Although the tetragonal phases have small relative As/P−As/P or $X-X$ interatomic distances, the orthorhombic phases have larger distances.

Introduction

The Landau theory of symmetry-breaking transitions allows determination of broken symmetries that occur with a change in temperature or composition. However, the complexity of the solid state enters when the required energetic stabilization of the distorted form is considered. Terms from band energy, Madelung energy and size effects can all be considered, and their complex interplay is generally difficult to analyze. The compounds considered here, because of the variation in chemical content (P/As substitutions, compounds containing Cu or Ag as the transition element) allow, with the aid of band structures and group theory, a partial unraveling of the factors important in the tetragonal to orthorhombic distortions in the $HfCuSi_2$-type structures.

Intermetallic compounds with 2D square nets of the main group elements are interesting because they often exhibit Peierls instabilities and undergo symmetry-breaking transitions (e.g., GdPS,[1] CeAsS,[2] $SrZnSb_2$,[3] $EuSb_2$,[4] $CaAl_4$,[5] $GdCuP_{2.20}$,[6] etc.). The reason for these distortions lies in the half filling of the widely dispersed bands centered on the main group elements. These broad bands, formed mainly by p_x and p_y orbitals, cross along some symmetry lines in the Brillouin zone and the Fermi level lies at the crossing: an ideal situation for a distortion and gap opening.[6,7] One of the prerequisites for a subsequent distortion is a separation of the valence band and the rare-earth d orbitals.[7] Even if these conditions are met, it is possible that a distortion does not occur; e.g., $EuSb_2$ ($CaSb_2$ type)[4] and $RECu_{1+\delta}P_{2+x}$[6,8,9] distort, but $YbSb_2$ ($ZrSi_2$ type)[10] and $RECuAs_2$[11] do not.

In the $RECuAs_{2-x}P_x$ series[6,8,9] the symmetry-breaking transitions are complicated and, as we show below, they cannot be characterized as mere consequences of a Peierls instability. The arsenides and some arsenophosphides adopt the tetragonal $HfCuSi_2$-type structure ($P4/nmm$ space group), which can be "continuously" distorted into the orthogonal $GdCuAs_{1.15}P_{0.85}$-type structure ($Pmmn$ space group) upon partial substitution of arsenic by phosphorus. This transition corresponds to a single irreducible representation and, according to Landau theory, can be continuous.[6,8] In the orthorhombic structures, the originally square As/P nets are slightly distorted: all distances within the As/P layers are the same, but the angles deviate from 90° (but by less than 1°). The band crossing still remains and electronic considerations in terms of the Peierls instability cannot explain the observed distortion. When nearly all of the arsenic in $RECuAs_{2-x}P_x$ is replaced by phosphorus, the orthorhombic structures distort further. In the phosphides $GdCuP_{2.20}$,[6] $ErCuP_2$[8] and $SmCu_{1.15}P_2$[9] the band crossing is avoided and their structures can be viewed as results of Peierls instabilities of the square nets of the phosphorus atoms.

The $RECuAs_2$ ($P4/nmm$ space group)[11] and $REAgAs_2$ ($Pmmn$ space group)[12] series have the As atoms in the square or nearly square nets, but in the case of the silver containing compounds the structures are distorted. Although it appears to be different from the As/P substitution in $RECuAs_{2-x}P_x$, the replacement of the smaller Cu atoms by the larger Ag atoms has the same effect on the structure. If one omits slight changes in the electronic structures and considers the structural aspect of the Cu/Ag replacement, it becomes obvious that the Ag atoms exert a matrix effect on the As atoms in the square net that is similar to that of the Cu atoms on the P atoms in the As/P layer.

In this paper, we combine the conclusions of Landau theory[6,8] with the electronic structures of the tetragonal and orthorhombic $RECuAs_{2-x}P_x$ phases to show that the continuous symmetry-breaking $P4/nmm \rightarrow Pmmn$ transitions are not caused by Peierls instabilities of the square As/P nets. Then we show that the distortions provide better packing and thus greater stabilization energy through a larger Madelung contribution. And finally, we generalize the results obtained for other known rare-earth copper and silver pnictides of the $REMX_2$ composition.

Band structure calculations were performed using the extended Hückel tight-binding (EHTB) method.[13] Lattice and atomic position parameters (Table 3) from the single-crystal

* To whom correspondence should be sent: 342 Spedding Hall, Ames Laboratory, Iowa State University, Ames, IA 50011, USA. E-mail: franzen@iastate.edu. Phone: (515) 294-5773. Fax: (515) 294-5718.

10.1021/jp0206018 CCC: $22.00
Published on Web 08/24/2002

TABLE 1: Parameters for the Extended Hückel Tight-Binding Calculations

atom	orbital	H_{ii}, eV, $GdCuAs_2$	H_{ii}, eV, GdCuAsP	ξ_1	c_1[a]	ξ_2	c_2[a]
Gd	6s	−7.61	−7.59	1.369	1.00		
Gd	6p	−5.03	−5.01	1.369	1.00		
Gd	5d	−8.05	−8.02	2.747	0.7184	1.267	0.4447
Cu	4s	−9.46	−9.11	2.20	1.00		
Cu	4p	−5.30	−5.03	2.20	1.00		
Cu	3d	−14.55	−14.00	5.95	0.5933	2.30	0.5744
As	4s	−16.22	−16.22	2.23	1.00		
As	4p	−12.16	−12.16	1.89	1.00		
P	3p		−18.60	1.75	1.00		
P	3p		−14.00	1.30	1.00		

[a] Coefficients used in the double-ζ Slater-type orbitals.

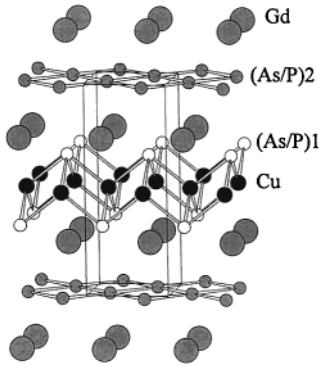

Figure 1. Structure of $GdCuAs_{1.15}P_{0.85}$ (*Pmmn* space group).

refinements of $GdCuAs_2$[6] were used in the calculations. The powder lattice parameters of GdCuAsP (a_{orth} = 3.8314(8), b_{orth} = 3.8443(8), c_{orth} = 9.8613(9) Å and V_{orth} = 142.25(4) Å^3) and atomic parameters of $GdCuAs_{1.15}P_{0.85}$[6] (Table 3) were taken for the calculation of the band structure and the total electronic energy of GdCuAsP. Because the As/P ratio is around 3/1 in the (As/P)2 net and is the inverse in the Cu(As/P)1 layer, a cell with a doubled *a* parameter was constructed to account for the As/P mixtures. A hypothetical tetragonal cell for GdCuAsP with $a_{tet} = b_{tet} = b_{orth} = 3.8443$, c_{tet} = 9.8613 Å and V_{tet} = 145.74 Å^3 was derived from the analysis of the lattice parameters of the tetragonal and orthorhombic phases in the *RE*$CuAs_{2-x}P_x$ series.[6,8,9] The atomic parameters for the tetragonal structure were assumed to be the same as for the orthorhombic one, but with $z = {}^1/_2$ for Cu and $z = 0$ for (As/P)2.

The orbital energies and coefficients for the Slater-type orbitals were taken from.[14] The parameters for Gd and Cu were refined by the alternating charge iteration technique, while the As and P parameters were kept constant (Table 1).

Structural Changes in *RE*$CuAs_{2-x}P_x$

Because the transitions between the arsenide and arsenophosphide structures are the same for the Sm, Gd, Ho and Er series, only the $GdCuAs_{2-x}P_x$ phases will be considered here. $GdCuAs_2$ has a tetragonal $HfCuSi_2$-type structure. Upon an As/P substitution this tetragonal structure distorts to an orthorhombic $GdCuAs_{1.15}P_{0.85}$-type structure[6] (Figure 1). Changes in symmetry and lattice parameters for $GdCuAs_{2-x}P_x$ are summarized in Table 2 and Figure 2. Table 3 gives the atomic parameters for $GdCuAs_2$ and $GdCuAs_{1.15}P_{0.85}$ obtained from the refinements of single-crystal data.[6] The structural changes are best visualized by viewing layers of the As2 and (As/P)2 atoms (Figure 3).

Upon the second-order transition (its nature is discussed below), the *a* and *b* parameters become slightly different, the maximum *b*/*a* ratio achieved is 1.0054(3). Because the

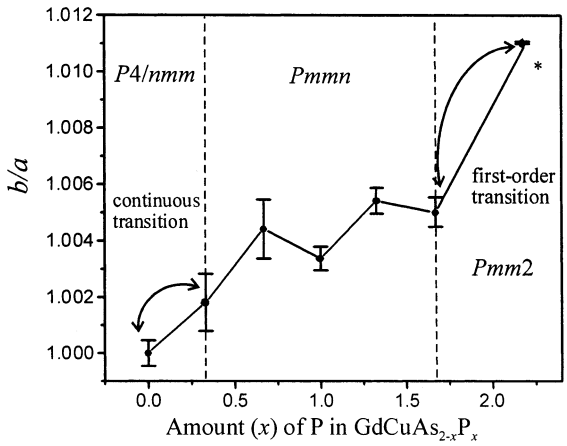

Figure 2. *b*/*a* ratio versus phosphorus amounts in $GdCuAs_{2-x}P_x$. Dashed lines show the experimentally established existence regions for the orthorhombic arsenophosphides. * Composition of the phosphide is $GdCuP_{2.16}$ (Rietveld refinement).

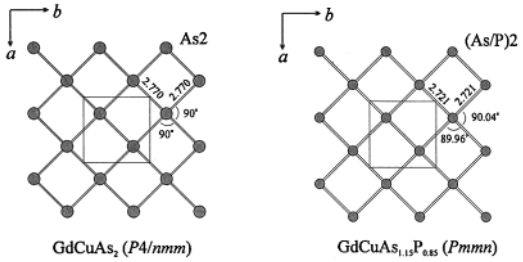

Figure 3. As and As/P layers in $GdCuAs_2$ and $GdCuAs_{1.15}P_{0.85}$.

(As/P)2 and Cu atoms move up and down from the horizontal planes, the 4-fold axis is lost. The (As/P2) and Cu shifts in $GdCuAs_{1.15}P_{0.85}$ are very small ($z_{As/P}$ = 0.000 05(11) and z_{Cu} = 0.499 89(12)), with the Cu shifts being larger. Similar small displacements are observed for refined orthogonal $HoCuAs_{0.99}P_{1.01}$,[8] $SmCu_{1.16}As_{0.86}P_{1.14}$[9] and $NdAgAs_2$,[12] but in the latter phase the As shifts are the largest and the Ag shifts are close to zero: z = 0.9955(6) for As2 and z = 0.5001(5) for Ag.

The structural distortions in $GdCuAs_{2-x}P_x$, as well as in $SmCuAs_{2-x}P_x$, $HoCuAs_{2-x}P_x$ and $ErCuAs_{2-x}P_x$, result when As atoms are substituted by smaller P atoms. If the P atoms are introduced in the square As layer a mismatch occurs between the optimal distances in the (As/P)2 layer and the *a*, *b* dimensions, determined by the matrix effect of the larger Cu atoms. This mismatch and its consequences are best characterized by the relative interatomic distances in the As/P net and this approach is presented in detail below ("Size Effect in *RE*$CuAs_{2-x}P_x$"). For smaller P atoms, the bonding would be optimized with shorter interatomic distances. Shorter interatomic distances for the P atoms in the structure lead to a smaller unit cell volume and an orthorhombic structural rearrangement.

To answer the question of whether the packing is optimized in this way, unit cell volumes of undistorted and distorted structures with the same composition must be compared. This direct comparison is impossible for the *P*4/*nmm* → *Pmmn* transition, which follows from the fact that a high-symmetry structure cannot be obtained below the transition temperature in the case of a displacive second-order structural transition. However, a tighter packing upon the *P*4/*nmm* → *Pmmn* transition can be inferred from the changes in the unit cell volume in the *RE*$CuAs_{2-x}P_x$ series (see "Size Effect in *RE*$CuAs_{2-x}P_x$").

TABLE 2: Powder Lattice Parameters for the $GdCuAs_{2-x}P_x$ Phases

composition	space group	*a*, Å	*b*, Å	*c*, Å	*b*/*a*	*V*, Å^3
$GdCuAs_2$	*P*4/*nmm*	3.9112(9)	3.9112(9)	9.930(3)	1	152.90(7)
$GdCuAs_{1.67}P_{0.33}$	*Pmmn*	3.883(2)	3.890(2)	9.908(4)	1.0018(7)	149.7(1)
$GdCuAs_{1.33}P_{0.67}$	*Pmmn*	3.850(2)	3.867(2)	9.888(4)	1.0044(7)	147.2(1)
GdCuAsP	*Pmmn*	3.8314(8)	3.8443(8)	9.8613(9)	1.0034(3)	145.25(4)
$GdCuAs_{0.67}P_{1.33}$	*Pmmn*	3.8072(9)	3.8278(9)	9.843(2)	1.0054(3)	143.44(6)
$GdCuAs_{0.33}P_{1.67}$	*Pmmn*	3.793(1)	3.812(1)	9.822(2)	1.0050(4)	142.01(6)
$GdCuP_{2.16}$[a]	*Pmm*2[b]	5.3284(1)	5.3868(1)	9.7487(3)	1.01096(3)	279.82(1)

[a] Composition from the Rietveld refinement. Composition from the single-crystal refinement is $GdCuP_{2.20}$. [b] Not a superstructure of $GdCuAs_{0.33}P_{1.67}$.

TABLE 3: Atomic Parameter for $GdCuAs_2$ (*P*4/*nmm* Space Group, $HfCuSi_2$ Type) and $GdCuAs_{1.15}P_{0.85}$ (*Pmmn* Space Group)

	$GdCuAs_2$				$GdCuAs_{1.15}P_{0.85}$			
atom		*x*	*y*	*z*		*x*	*y*	*z*
Gd	2*c*	1/4	1/4	0.23844(8)	2*a*	1/4	1/4	0.24108(4)
Cu	2*b*	3/4	1/4	1/2	2*b*	1/4	3/4	0.49989(12)
*X*1[a]	2*c*	1/4	1/4	0.65810(18)	2*a*	1/4	1/4	0.65545(16)
*X*2[b]	2*a*	3/4	1/4	0	2*b*	1/4	3/4	0.00005(11)

[a] *X*1 = 32.8(8)%As + 67.2(8)%P for $GdCuAs_{1.15}P_{0.85}$. [b] *X*2 = 82.1(6)%As + 17.9(6)%P for $GdCuAs_{1.15}P_{0.85}$.

TABLE 4: One-Dimensional Irreducible Representation B_{1g} of *P*4/*nmm* at Γ

g	ϵ	C_{4z}	C_{4z}^3	C_{2z}	C_{2x}	C_{2y}	$C_{2(x+y)}$	$C_{2(x-y)}$
$\chi(g)$	1	−1	−1	1	1	1	−1	−1
g	*i*	$\bar{C}_{4z}$	$\bar{C}_{4z}^3$	σ_z	σ_x	σ_y	σ_{x+y}	σ_{x-y}
$\chi(g)$	1	−1	−1	1	1	1	−1	−1

Symmetry-Breaking Transitions *P*4/*nmm* → *Pmmn* in Terms of Landau Theory

The continuous symmetry-breaking transitions *P*4/*nmm* → *Pmmn* in the $GdCuAs_{2-x}P_x$,[6] $HoCuAs_{2-x}P_x$, $ErCuAs_{2-x}P_x$,[8] and $SmCuAs_{2-x}P_x$[9] series do not create a superstructure. We will analyze only the $GdCuAs_{2-x}P_x$ case (Figure 2, Table 2), but the results obtained can be equally applied to other *RE*$CuAs_{2-x}P_x$ series. Because no translation is lost during the distortions, the **k** vector to which the distortions correspond is $k = 0$ and the irreducible representations are isomorphous with those of the point group D_{4h} for $GdCuAs_2$.

One of the considerations of Landau theory[15−17] is that a continuous symmetry-breaking transition must correspond to a single irreducible representation (IR). There are eight one- and two two-dimensional IRs at $k = 0$. The two-dimensional representations would result in distorted structures with 4 symmetry elements, corresponding to monoclinic centrosymmetric or orthorhombic noncentrosymmetric subgroups, which are not the case here, and therefore, they are not of interest. All one-dimensional representations, except the totally symmetric one, result in a loss of all symmetry operations with character −1, and they, accordingly, lead to a halving of the number of the rotational symmetry elements, and thus to space groups with eight essential symmetry elements. Four of the seven subgroups have orthorhombic unit cells, but only two (from the B_{1g} and B_{2g} representations) preserve the horizontal plane and inversion center. The space group *Pmmn*, corresponding to B_{1g} (Table 4), is the one found experimentally in $GdCuAs_{1.15}P_{0.85}$.

For a transition to be continuous an expansion of the Gibbs free energy in the order−disorder parameter, η, should not contain any third-order combination of the basis functions. In the case of the one-dimensional irreducible representation B_{1g}, a basis function is symmetric to one-half and antisymmetric to the other half of the symmetry elements. Thus, no third-order invariant can be formed and the *P*4/*nmm* → *Pmmn* transition with $a_{ort} = a_{tet}$, $b_{ort} = b_{tet}$ and $c_{ort} = c_{tet}$ follows the Landau conditions for a second-order phase transition.

The last criterion, which must be met for a second-order phase transition from $GdCuAs_2$ (*P*4/*nmm*) to $GdCuAs_{1.15}P_{0.85}$ (*Pmmn*), is the Lifshitz criterion. It requires a minimum in the Gibbs free energy to be fixed by the symmetry at the **k** vector corresponding to the transition. This condition prevents a decrease of the Gibbs free energy with a change of the **k** vector and, therefore, excludes the possibility of continuous distortion to a modulated structure. In the case under consideration inversion symmetry is in the point group of the wave vector and thus the reciprocal space point meets the Lifshitz criterion.

Landau Theory and Bonding for the *P*4/*nmm* → *Pmmn* Transitions

Imposing the constraint of correspondence of a second-order transition to a single irreducible representation, Landau theory determines, in this way, the symmetry of the normal mode (lattice vibration) that leads to the distortion. In our case, the symmetry of the normal mode involved in the *P*4/*nmm* → *Pmmn* distortion is B_{1g}. Although Landau theory is of use in describing the nature of transitions, it cannot, however, explain the electronic or geometric factors causing these symmetry-breaking transitions.

Because the band structure of $GdCuAs_2$ (*P*4/*nmm*) (Figure 4) has widely dispersed bands that cross each other, and the Fermi level lies at the crossing, at first it appears that a Peierls instability can lead to the observed *P*4/*nmm* → *Pmmn* distortions. This electronic instability resulting in the symmetry breaking is associated with a strong interaction of electronic states through the B_{1g} normal mode. In general, it is possible that this interaction results in a gap opening at the Fermi level (a first-order Peierls distortion) or in changes in energy of the states below and above the Fermi level without opening a gap (a second-order Peierls distortion). In each case, the energy of the system would be lowered and the crystal symmetry reduced. The two distortion types and energetic gains associated with them are considered below.

Electronic States of $GdCuAs_2$ and B_{1g} Normal Mode

Electronic states involved in mixing through the B_{1g} normal mode are those for which the direct product of their irreducible representations contains the irreducible presentation B_{1g}. Group theoretical analysis shows that the B_{1g} normal mode is associated with vibrations of the Cu and As2 atoms and, therefore, that electronic states of the Cu or As2 must be involved in the interaction (here, we have assumed no P in the structure). Also, the mixing states must occur above and below the Fermi level to give an energy gain upon distortion and the energy separation between them should be small because the strength of orbital mixing is inversely proportional to the energy difference

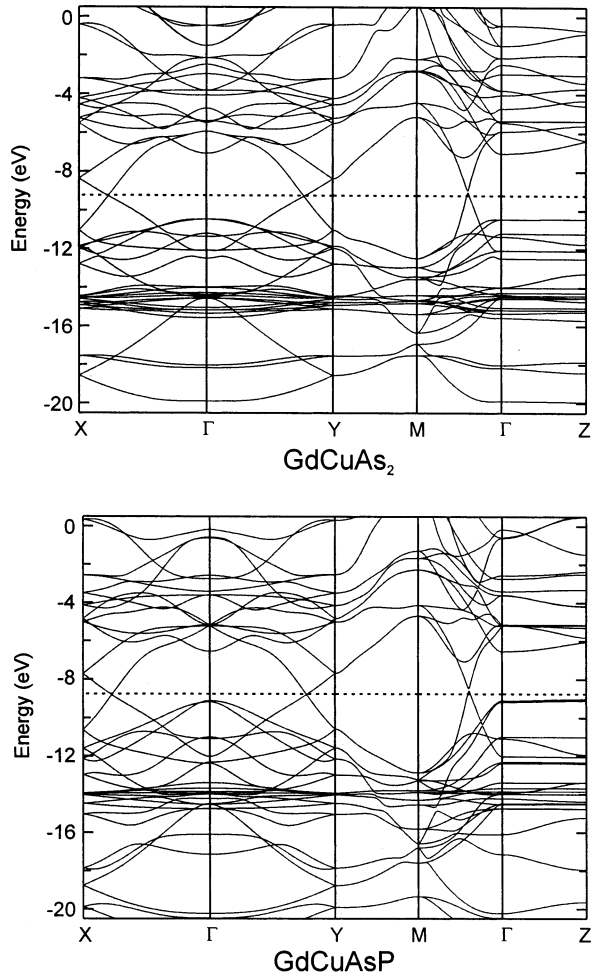

Figure 4. Band structures of $GdCuAs_2$ (*P*4/*nmm* space group) and GdCuAsP (*Pmmn* space group). Here, in GdCuAsP the *X*1 site is occupied only by P and the *X*2 site is occupied only by As.

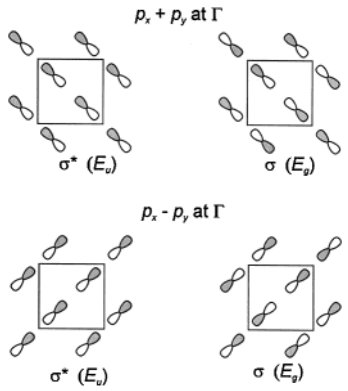

Figure 5. Molecular orbitals (MOs) from the p_x and p_y orbitals of the As2 atoms and their symmetries at Γ.

between them. Thus, we need to consider only bands in the vicinity of the Fermi level for $GdCuAs_2$ (Figure 4).

Using an orbital picture, symmetry of the bonding and antibonding As2 molecular orbitals at the Γ point can be easily deduced (e.g., p_x and p_y orbitals in Figure 5). The orbital interaction leading to formation of these MOs and their relative energies at the Γ point are presented in Figure 6. Here, we assume a negative charge for the As2 atoms in order to have the correct filling of the states. A delocalized picture, showing the change in energy of the As2 states along the symmetry lines

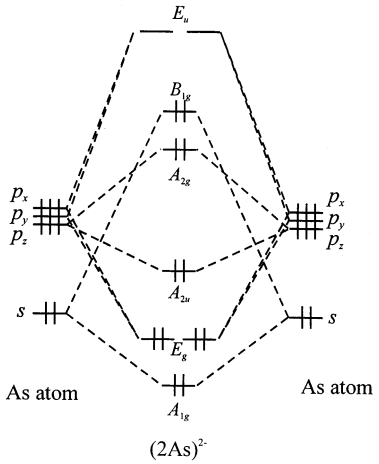

Figure 6. Symmetries of the MOs formed from the As2 orbitals and their relative energies at Γ. As atoms have one additional electron.

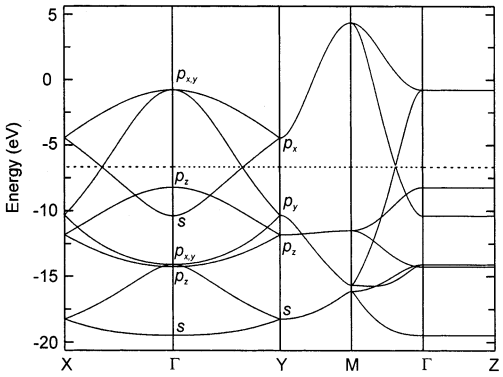

Figure 7. Calculated band structure of the $(As2)^-$ layer of tetragonal $GdCuAs_2$ and orbital character of the states at Γ and *Y*.

in the first Brillouin zone, is given in Figure 7. There is a crossing of two bands and the Fermi level falls exactly at the crossing. States at the crossing have the largest contribution from the As2 p_x and p_y orbitals. These bands are also the ones that cross at the Fermi level in the complete band structure of $GdCuAs_2$ and that is why they are considered in detail here. However, the crossing of the bands and associated Peierls instability does not lead to the observed orthorhombic distortion at $k = 0$ since the direct product ($E_g \otimes E_u = A_{1u} + A_{2u} + B_{1u} + B_{2u}$) of the irreducible representations of the As2 antibonding $p^*_{x,y}$ and bonding $p_{x,y}$ orbitals does not contain the B_{1g} representation that corresponds to the observed transition from $GdCuAs_2$ to $GdCuAs_{1.15}P_{0.85}$. Thus, the $p_{x,y}$ bands do not mix and the crossing remains (Figure 4).

On the other hand, the mixing of the As2 p^*_z molecular orbitals (B_{1g} symmetry), that are below the Fermi level, with the Gd *s* or d_{z^2} molecular orbitals (A_{1g} symmetry), that are above, is allowed through the normal mode B_{1g} at the Γ point. This normal mode is associated with vibration of the As2 atoms as shown in Figure 8a. Also allowed is a mixing between the Cu p^*_z, *s** MOs (B_{1g}, A_{2u} symmetries) with the As1 *s* and p_z MOs (A_{1g}, B_{2u} symmetries), respectively, through the B_{1g} mode, which now is attributed to the Cu vibrations (Figure 8b). There are some other states coupled through the B_{1g} modes, but all the states can be divided into two groups: those that are coupled through the As2 vibrations and the others that are coupled through the Cu vibrations.

From the EHTB calculations on GdCuAsP the displacements of the Cu and (As/P)2 atoms from their positions in the tetragonal structure do not change the total electronic energy.

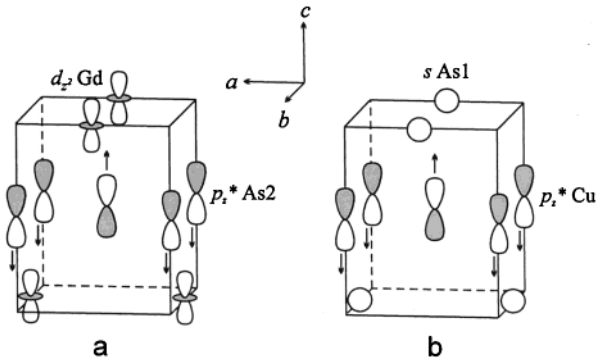

Figure 8. Allowed interactions through the B_{1g} normal mode (a) of the As2 atoms between the Gd d_z2 and As2 p_z* orbitals, (b) of the Cu atoms between the As1 *s* and Cu p_z* orbitals at Γ.

For this calculation, the unit cell was assumed to be tetragonal, but the Cu and (As/P)2 fractional coordinates were those in the real orthorhombic structure. In all calculations, one P and one As atom were introduced into the As2 and CuP1 layers, respectively. When the structure is orthorhombicly distorted, with the Cu and (As/P)2 atoms being at their real displaced positions, the total electronic energy for GdCuAsP (−352.80 eV per unit formula) becomes even slightly larger than that for the hypothetical tetragonal structure (−352.81 eV). It must be remembered that the atomic arrangement of the tetragonal GdCuAsP structure is based on that of the orthorhombic one and in the real tetragonal phase, if it can be obtained at all, the atomic parameters can be somewhat different and the electronic energy of this tetragonal structure can therefore be even smaller. It is thus clear that the electronic energy is not lowered through a second-order Peierls distortion, but it is also clear that the orthorhombic structure is more stable, and that this stability originates with introduction of P atoms.

Size Effect in *RE*CuAs$_{2-x}$P$_x$

As alluded to above, the size of the P atoms could be related to the distortion from the tetragonal to orthorhombic structures in SmCuAs$_{2-x}$P$_x$, GdCuAs$_{2-x}$P$_x$, HoCuAs$_{2-x}$P$_x$, and ErCuAs$_{2-x}$P$_x$; the smaller P atoms tend to stabilize the GdCuAs$_{1.15}$P$_{0.85}$-type structures. Because the vibrational mode B_{1g} responsible for the *P*4/*nmm* → *Pmmn* distortion is associated with the (As/P)2 and Cu nets, it is natural to confine our attention to these two nets. To go beyond a qualitative structural description of the transitions and to have a quantitative criterion for analyzing stability of the tetragonal *REMX*$_2$ structures, we introduce a *relative interatomic distance* for the *M* and *X* nets. A relative interatomic distance is the ratio between the *X*−*X* or *M*−*M* interatomic distances projected onto the *ab* plane and the element diameters [We use the element radii/diameters for Cu, As, and P because four of their nearest neighbors are atoms of the same type. Besides, the charges on Cu, As, and P in the Cu and As/P layers are small, as determined from the analysis of the atomic orbital population for GdCuAsP].

In tetragonal GdCuAs$_2$ and other rare-earth copper arsenides, the Cu net is structurally the same as the As2 layer. The element radii of the As and Cu atoms are close: 1.245 and 1.278 Å, respectively. So, the relative interatomic distances *r*/*d* in the horizontal As2 and Cu layer are similar in the tetragonal GdCuAs$_2$ phase ($r_{As-As}/d_{As} = 1.111$ and $r_{Cu-Cu}/d_{Cu} = 1.082$). When smaller P atoms (radius is 1.105 Å for the white modification) are introduced in the As2 square net, the relative interatomic distance for P becomes significantly larger than those for As and Cu and, accordingly, the P atom environment is unfavorable (in GdCuAsP $r_{As}/d_{As} = 1.090$, $r_{Cu-Cu}/d_{Cu} = 1.062$ and $r_{P-/P}/d_P = 1.228$).

There are two ways, consistent with the B_{1g} normal mode, to increase packing and more effectively bind the P atoms in the structure. One would be to move the (As/P)2 out of the horizontal plane at $z = 0$ (normal mode B_{1g} in Figure 8a) and closer to the Gd atoms, but leave the copper atoms in the original positions. The relative interatomic distance for Cu atoms would not change and they would dictate the unit cell dimensions in the *ab* plane. Although there is no experimental proof, it is reasonable to conclude that this kind of structural adaptation would have small or no effect on the *a*, *b* parameters but would decrease the *c* parameter. The second possibility is to keep the As/P atoms in the plane but to move Cu atoms out of the horizontal plane at $z = {}^1/_2$ (normal mode B_{1g} in Figure 8b) thereby decreasing the relative Cu−Cu interatomic distance projected on *this plane* in order to match the smaller relative (As/P)2−(As/P)2 interatomic distance in the plane at $z = 0$. In the second case the *a* and/or *b* parameters would decrease upon the *P*4/*nmm* → *Pmmn* transition. This type of structural adaptation is believed to occur in the *RE*CuAs$_{2-x}$P$_x$ series as judged from the larger shifts of the Cu atoms in the orthorhombic arsenophosphides and from the lattice parameters of the two samarium phases with close As/P ratios across the transition point: SmCuAs$_{1.22}$P$_{0.78}$, *P*4/*nmm*, $a = b = 3.8863(8)$, $c = 9.919(2)$ Å and SmCuAs$_{1.11}$P$_{0.89}$, *Pmmn*, $a = 3.8659(8)$, $b = 3.8816(8)$, $c = 9.913(2)$ Å.[9] In both cases, due to the B_{1g} normal mode the C_{4z} axis is lost and the *P*4/*nmm* symmetry is reduced to *Pmmn*.

EHTB calculations of the total electronic energy for the undistorted and distorted (As/P)2$^-$ and (Cu(As/P)1)$^{2-}$ layers in GdCuAsP support the orthorhombic distortion due to the B_{1g} shifts of the Cu atoms. The (As/P)2 and Cu displacements are both energetically unfavorable ($\Delta E_{el} > 0$), but the B_{1g} shifts of the (As/P)2 atoms ($z_{As/P} = 0.000\,05$) are more energetically unfavorable ($\Delta E_{el} = 0.05$ eV) than those of the Cu atoms ($z_{Cu} = 0.499\,89$) in the (Cu(As/P)1)$^{2-}$ units ($\Delta E_{el} = 0.03$ eV). Thus, from the experimental and theoretical data it can be concluded that in the orthorhombic *RE*CuAs$_{2-x}$P$_x$ phases it is the Cu layer that changes to be compatible with the more compact As/P layer and undergoes the distortion.

Because the electronic factors do not drive the *P*4/*nmm* → *Pmmn* transition, geometric factors with associated Madelung energies are most probably important in the distortion. A role of the latter factors can be traced through a volume decrease upon the transition that leads to a better packing and larger Madelung energy stabilization. Although indirectly, a volume decrease can be inferred from changes of the unit cell volume in the *RE*CuAs$_{2-x}$P$_x$ series. As seen in Figure 9, there is a step down in the slope of the unit cell volume upon the *P*4/*nmm* → *Pmmn* transition in SmCuAs$_{2-x}$P$_x$ and ErCuAs$_{2-x}$P$_x$. This cannot be said about GdCuAs$_{2-x}$P$_x$ because there is only one data point for the tetragonal phase. In the HoCuAs$_{2-x}$P$_x$ series there is a change in the slope upon the distortion. These steps in SmCuAs$_{2-x}$P$_x$ and ErCuAs$_{2-x}$P$_x$ indicate clearly that an increase in packing is the structural response to the smaller P atoms.

To compare the Madelung energies of the tetragonal and distorted orthorhombic GdCuAsP structures we used a simple ionic picture based on an electron count in GdCuAsP. The Gd atoms have no short metal−metal bonds and therefore may be counted as Gd^{3+} in agreement with the results of the magnetic susceptibility measurements for GdCuAs$_2$ and GdCuP$_{2.20}$.[6] The (As/P)1 atoms have no close anion neighbors and can be assumed (As/P)$^{3-}$. The shortest Cu−Gd and Cu−Cu distances

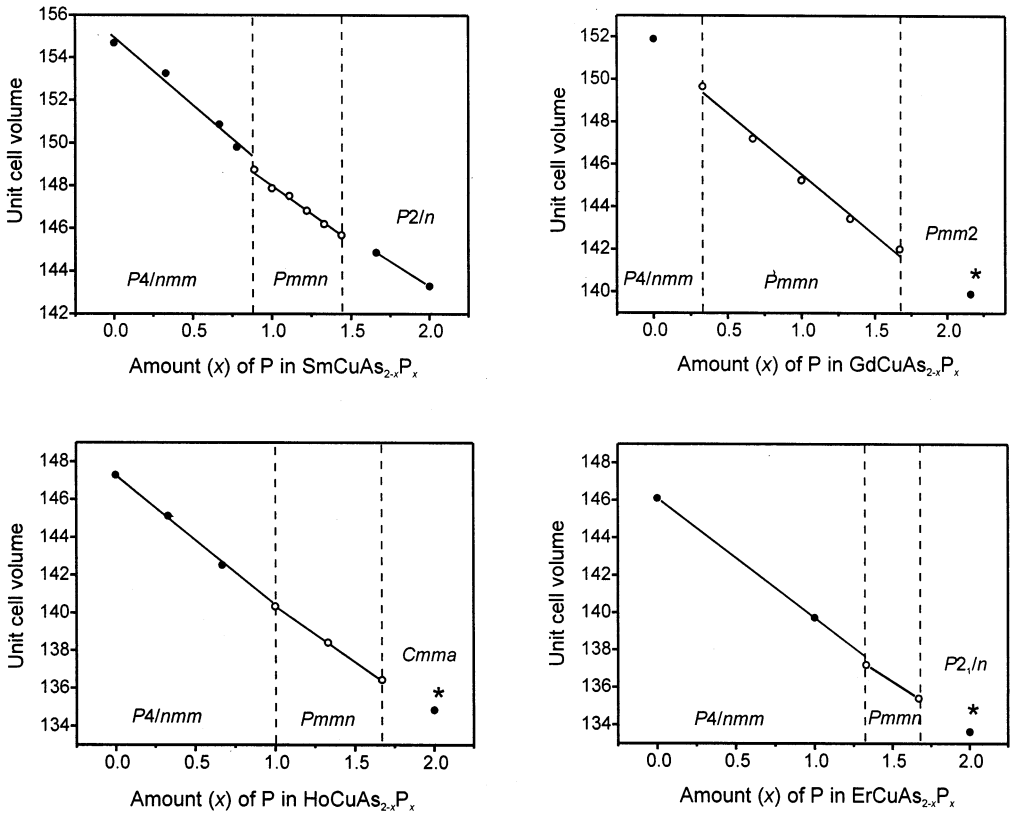

Figure 9. Unit cell volume versus phosphorus amount in the *RE*CuAs$_{2-x}$P$_x$ series. Dashed lines show the experimentally established existence regions for the orthorhombic arsenophosphides (open circles). Discontinuity in the unit cell volume curves during the *P*4/*nmm* → *Pmmn* distortions is artificially produced (not real) to illustrate the steps in the slopes. * $^1/_2V_{\text{unit cell}}$. For the Gd series the composition of the phosphide is GdCuP$_{2.16}$.

are 3.1986−3.1995 and 2.7211 Å in the real GdCuAs$_{1.15}$P$_{0.85}$ structure.[6] The copper distances are typical for Cu^+ (d^{10}) as usually found in pnictide and chalcogenide systems. On the basis of the above oxidation state assignments, the electronic structure can be described as $(Gd^{3+})(Cu^+)((As/P)1^{3-})((As/P)2^-)$. Although this formula does not represent the real charge distribution in the unit cell, it is suitable for an analysis of the sign of the change in Madelung energy (ΔE_{ion}). Calculations show that E_{ion} for the orthorhombic structure (−85.87 eV per unit cell) is slightly lower than E_{ion} for the hypothetical tetragonal structure (−85.80 eV). It is obvious that the energetic gain upon the *P*4/*nmm* → *Pmmn* transition is, as it should be for a second-order transition considered in this way, rather small, but this energetic stabilization, originating with the introduction of the smaller P atoms, leads to the orthorhombic distortion in GdCuAsP.

Reverse *Pmmn* → *P*4/*nmm* Transition

The *P*4/*nmm* → *Pmmn* distortions in the *RE*CuAs$_{2-x}$P$_x$ series are structural adaptations to small P atoms. The B_{1g} normal mode of the Cu1 atoms provides a tighter environment for the P2 atoms through making the unit cell parameters smaller in the *ab* plane. Another way to bind the P atoms tightly in the structure would be to have some additional atoms around the (As/P)2 layer and in the tetragonal antiprisms made of the (As/P)2 and *RE* atoms. Two obvious requirements that must be met in this case are the size of the additional atoms and the size of the void, which depends on the rare-earth element. Provided that no new element is introduced into the structure, only copper atoms are most likely to go into the voids. The rare-earth atoms are too large and phosphorus or arsenic is unlikely be in that place due to the repulsion between the negatively charged P or As atoms. Among the studied phases, the *RE*CuAs$_{2-x}$P$_x$ series (*RE* = Sm, Gd, Ho, and Er), the samarium copper arsenophosphides have the largest voids and, therefore, could take some extra copper into their structures. Indeed, we were successful to introduce additional Cu atoms into the structure of a samarium arsenophosphide and restabilize the tetragonal structure through the reverse *Pmmn* → *P*4/*nmm* transition.[9] SmCuAs$_{0.67}$P$_{1.33}$ adopts the orthorhombic structure (*Pmmn*), whereas SmCu$_{1.1}$As$_{0.67}$P$_{1.33}$ and SmCu$_{1.2}$As$_{0.67}$P$_{1.33}$ are both tetragonal (*P*4/*nmm*).

The concept of the relative interatomic distance was helpful in understanding stability of some SmCuAs$_{2-x}$P$_x$ phases. The relative interatomic distances in the tetragonal samarium arsenophosphides SmCuAs$_{2-x}$P$_x$ with $0 < x < 0.78$ were found to be too large for these phases to remain tetragonal[9] (the borderline in *r*/*d* between the tetragonal and orthorhombic phases is discussed below). Additional Cu atoms were assumed in their structures and they were believed to stabilize these tetragonal structures. X-ray diffraction experiments performed on crystals from the SmCuAs$_{1.67}$P$_{0.33}$ sample proved small excess of Cu in their tetragonal structure (see the structure of SmCu$_{1.05}$As$_{1.67}$P$_{0.33}$ in Figure 10). As expected, the additional copper atoms are around the (As/P)2 layer.

Role of the *M* and *X* Elements in *REMX*$_2$

In *RE*CuAs$_{2-x}$P$_x$, the *P*4/*nmm* → *Pmmn* distortions occur when the relative interatomic distances in the (As/P) layer become smaller than those in the Cu layer. If this size argument is correct, then a similar trend would be observed for other rare-earth transition metal pnictides. Here, we consider known rare-earth copper or silver phosphides, arsenides and antimonides. The antimonides and copper arsenides have the

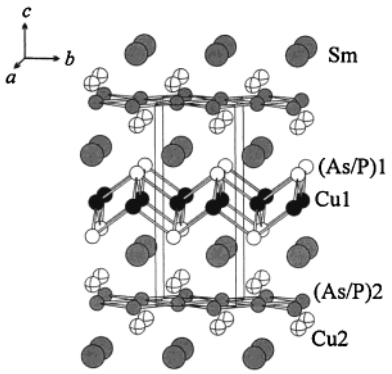

Figure 10. Structure of $SmCu_{1.05}As_{1.67}P_{0.33}$ (*P*4/*nmm*). Occupancy for the Cu2 site is 4.6(6)%.

tetragonal $HfCuSi_2$ structure while other phases adopt distorted variants of the $HfCuSi_2$ structure. For the analysis, we use lattice parameters and compositions for *RE*$AgSb_2$ from,[11,18] for *RE*$CuSb_2$ from,[19] for *RE*$CuAs_2$ and *RE*$Cu_{1+x}As_2$ from,[11,20] for *RE*$AgAs_2$ from,[12] for *RE*$CuAs_{2-x}P_x$ and *RE*CuP_2 from.[6,8,9] The formula *RE*CuP_2 is used here for simplicity and does not represent the actual compositions of the different phosphides, e.g., $SmCu_{1.15}P_2$,[9] $GdCuP_{2.20}$,[6] $HoCuP_2$ and $ErCuP_2$.[8] Furthermore, the phosphides have larger distortions in the P layer compared to those in the (As/P) layers of orthorhombic *RE*$CuAs_{2-x}P_x$ and their structural description is beyond the scope of this paper.

Figure 11 shows the relative interatomic distances r_{x-x}/d_x in the *X* layer of the $REMX_2$ pnictides (*RE* = rare earth; *M* = Cu, Ag; *X* = P, As, Sb). For the orthorhombic structures, these are the distances projected on the *ab* plane; and for the pure phosphides, they are the average projected distances. For the copper and silver antimonides, the relative Sb−Sb interatomic distances are around 1.05. The two plots nearly overlap, which means that the *a* and *b* parameters are determined by the size of the Sb atoms and that the Sb atoms are practically in contact. For the arsenide, the *RE*$CuAs_2$ and *RE*$AgAs_2$ graphs are now well separated: the size of the Cu and Ag atoms starts to dictate unit cell dimensions in the *ab* plane.

As the relative *X*−*X* interatomic distances increase and become close to 1.13, the tetragonal structures undergo orthorhombic distortions. The reason for the change is that the *X*−*X* distance, which now depends on the *M* layer, is much larger than the diameter of the *X* atoms (i.e., relative *X*−*X* interatomic distances become larger), and the structures distort to adapt to the smaller *X* atoms. In *RE*$CuAs_{2-x}P_x$ full substitution of As atoms by P makes the *X* layer (As/P layer) even less dense and around $r_{x-x}/d_x = 1.20$, the orthorhombic structures undergo further distortions.

In Figure 11, the tetragonal structures are represented by solid symbols, the orthorhombic structures by open ones and the structures of the phosphides by symbols with a cross. There is a separation between the tetragonal and orthorhombic structures and between the orthorhombic structures and the further distorted structures of the phosphides. Interestingly, the tetragonal copper arsenides of La, Ce and Pr, for which $r_{x-x}/d_x > 1.13$, have additional Cu atoms around the As layer.[20] Tetragonal *RE*$CuAs_2$ of the smaller rare-earth elements have not been reported to accommodate interstitial atoms.[11,20] It can be assumed that due to the large rare-earth atoms the relative As−As interatomic distances increase above the stability limit and the tetragonal structures of La, Ce, and Pr can either distort to improve the packing or take in some additional atoms to more efficiently fill the space. The structures of La, Ce, and Pr follow a second path ($LaCu_{1.23(1)}As_2$, $CeCu_{1.01(1)}As_2$, and $PrCu_{1.09(1)}As_2$) and preserve the tetragonal symmetry.

All known *RE*$AgAs_2$ structures except tetragonal $LaAgAs_2$ and $CeAgAs_2$ [12] are orthorhombicly distorted as expected from their r_{x-x}/d_x values. On the basis of the Cu interstitials in $LaCu_{1.23(1)}As_2$, $CeCu_{1.01(1)}As_2$ and $PrCu_{1.09(1)}As$ and the r_{x-x}/d_x data, the $LaAgAs_2$ and $CeAgAs_2$ structures are likely to have additional Ag atoms around the As layer. Single-crystal refinements are needed to test this argument. In the refined $NdAgAs_2$ structure the As2 displacements ($z = 0.9955(6)$) from the horizontal plane are larger than those of Cu ($z = 0.5001(5)$).[12] It is likely that the B_{1g} normal mode of the As2 atoms, and thus rearrangement of the As layer, play the key role in the *P*4/*nmm* → *Pmmn* distortion of *RE*$AgAs_2$.

The $REMX_2$ structures undergo orthorhombic distortions to increase packing in the smaller *X* layer. However, in the distorted structures, the relative *X*−*X* interatomic distances are still large and the *X* atoms are not in contact, although bringing them into

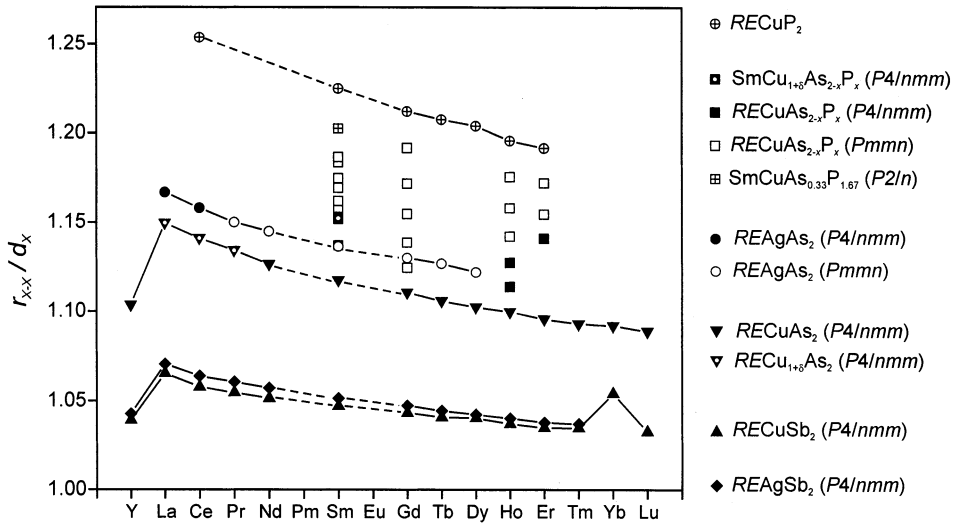

Figure 11. Relative interatomic distance r_{x-x}/d_x in $REMX_2$. r_{x-x}/d_x is the ratio between the average *X*2−*X*2 distance projected on the *ab* plane and the element diameter of *X*. For *RE*$CuAs_{2-x}P_2$ the diameter d_x is the sum of the As and P radii weighted by the composition. The solid symbols denote the tetragonal $HfCuSi_2$-type structures, the open symbols represent the orthorhombic $GdCuAs_{1.15}P_{0.85}$-type structures, and the symbols with a cross represent the further distorted structures.

closer proximity was the driving force for the symmetry-breaking transitions. These preserved large $X-X$ separations show a complex interplay of electronic and geometric factors determining phase stability and, obviously, the orthorhombic structures are compromises in this interplay. So far, the lanthanide contraction was not considered. As judged from the slope of the lines in Figure 11, its role is not important for *RE*$AgSb_2$ and *RE*$CuSb_2$. On the other hand, in the series with smaller *M* or *X* atoms the size of a rare earth starts to have an increased effect on the unit cell dimensions. The structural aspect of this increased influence can be seen in $GdCuAs_{2-x}P_x$, $HoCuAs_{2-x}P_x$, and $ErCuAs_{2-x}P_x$.[6,8] As the size of the rare-earth atom decreases, distortions from the tetragonal to orthorhombic structures are shifted to higher phosphorus concentrations.

Recently, Seo and Corbett analyzed the factors causing the $SrIn_4$ phase to adopt the monoclinic $EuIn_4$ structure instead of the tetragonal $BaAl_4$-type.[21] The tetragonal $HfCuSi_2$ structure, in which the rare-earth copper or silver pnictides crystallize, can be derived from $BaAl_4$, or vice versa. Seo and Corbett showed that the geometric factors, not electronic ones, and the associated Madelung energy dictate the structures of $SrIn_4$ and $EuIn_4$. Monoclinic structures provide better packing for the Eu^{2+}, Sr^{2+} ions and the In_4^{2-} network, whereas the tetragonal structure is optimal for the larger Ba^{2+} ions. In $REMX_2$, we observe a similar size effect although distortions are different and less drastic.

Conclusions

Application of Landau theory to the $P4/nmm \rightarrow Pmmn$ distortions in the *RE*$CuAs_{2-x}P_x$ series showed that the transitions correspond to the one-dimensional irreducible representation B_{1g} and can be continuous. It was shown from group theoretical considerations that these symmetry-breaking transitions are not caused by Peierls instabilities of the square As/P nets: mixing of the crossing bands is not possible through the B_{1g} normal mode. Although second-order Peierls distortions of the tetragonal $HfCuSi_2$-type structures to the orthorhombic $GdCuAs_{1.15}P_{0.85}$-type structures are compatible with the B_{1g} vibration, there is no electronic energy gain upon the distortions, and thus, this kind of instability is very unlikely to be a key factor in the transitions.

The $P4/nmm \rightarrow Pmmn$ distortions in *RE*$CuAs_{2-x}P_x$ and the structures of *RE*$AgAs_2$ are most likely to be the results of a subtle structural adaptation to the relative sizes of the given atoms. Introducing smaller P atoms in the As layer or replacing the Cu atoms by the larger Ag atoms create mismatches between sizes of the As/P and Cu or Ag layers. Now, better packing is achieved through the atomic rearrangements, mainly through the B_{1g} shifts of the Cu atoms in *RE*$CuAs_{2-x}P_x$ and As atoms in *RE*$AgAs_2$.

In $REMX_2$, a relative interatomic distance in the square net of a main group element *X* can be used to characterize the mismatch between the *X* and *M* layers. If tetragonal *RE*$CuSb_2$, *RE*$AgSb_2$, and *RE*$CuAs_2$ lie below the imaginary borderline, *RE*$AgAs_2$, *RE*$CuAs_{2-x}P_x$, and *RE*CuP_2 have larger relative $X-X$ interatomic distance and undergo distortions.

Acknowledgment. This research was supported by the Office of the Basic Energy Sciences, Materials Sciences Division, US Department of Energy, DOE. The Ames Laboratory is operated for DOE by Iowa State University under Contract No. W-7405-Eng-82.

References and Notes

(1) Hulliger, F.; Schmelczer, R.; Schwarzenbach, D. *J. Solid State Chem.* **1977**, *21*, 371−374.

(2) (a) Sfez, G.; Adolphe, C. *Bull. Soc. Fr. Mineral. Cristallogr.* **1972**, *95*, 553−557. (b) Ceolin, R.; Rodier, N.; Khodadad, P. *J. Less-Common Met.* **1977**, *53* (1), 137−140.

(3) Brechtel, E.; Cordier, G.; Schäfer, H. *Z. Naturforsch., B: Anorg. Chem., Org. Chem.* **1979**, *34B*, 251−255.

(4) Hulliger, F.; Schmelczer, R. *J. Solid State Chem.* **1978**, *26*, 389−396. (b) Wittmann, M.; Schmettow, W.; Sommer, D.; Bauhofer, W.; von Schnering, H. G. In *Solid Compounds of Transition Metals VI, International Conf.*; Stuttgart, 1979; p 217.

(5) Miller, G. J.; Li, F.; Franzen, H. F. *J. Am. Chem. Soc.* **1993**, *115*, 3739−3745.

(6) Mozharivskyj, Y.; Kaczorowski, D.; Franzen, H. F. *J. Solid State Chem.* **2000**, *155*, 259−272.

(7) Tremel, W.; Hoffmann, R. *J. Am. Chem. Soc.* **1987**, *109*, 124−140.

(8) Mozharivskyj, Y.; Kaczorowski, D.; Franzen, H. F. *Z. Anorg. Allg. Chem.* **2001**, *627*, 2163−2172.

(9) Mozharivskyj, Y.; Pecharsky, A. O.; Bud'ko, S. L.; Franzen, H. F., submitted to *Z. Anorg. Allg. Chem.*

(10) Bodnar, R. E.; Steinfink, H. *Inorg. Chem.* **1967**, *6*, 327−330.

(11) Brylak, M.; Möller, M. H.; Jeitschko, W. *J. Solid State Chem.* **1995**, *115*, 305−308.

(12) Demchyna, R. O.; Kuz'ma, Y. B.; Babizhetsky, V. S. *J. Alloys Compd.* **2001**, *315*, 158−163.

(13) Ren, J.; Liang, W.; Whangbo, M.-H. *Crystal and Electronic Structure Analyser (CAESAR)*; North Carolina State University: Raleigh, North Carolina, 1998.

(14) Alvarez, S. *Table of Parameters for Extended Hückel Calculations*; Barcelona, 1987.

(15) Landau, L. D.; Lifshits, E. M. *Statistical Physics*; Pergamon Press: London, 1958; Vol. 5.

(16) Franzen, H. F. *Physical Chemistry of Solids*; World Scientific: Singapore, 1994.

(17) Franzen, H. F. *Chem. Mater.* **1990**, *2*, 486−491.

(18) Sologub, O.; Noël, H.; Leithe-Jasper, A.; Rogl, P.; Bodak, O. I. *J. Solid State Chem.* **1995**, *115*, 441−446.

(19) Sologub, O.; Hiebl, K.; Rogl, P.; Noël, H.; Bodak, O. *J. Alloys Compd.* **1994**, *210*, 153−157.

(20) Wang, M.; McDonald, R.; Mar, A. *J. Solid State Chem.* **1999**, *147*, 140−145.

(21) Seo, D.-K.; Corbett, J. D. *J. Am. Chem. Soc.* **2000**, *122*, 9621−9627.